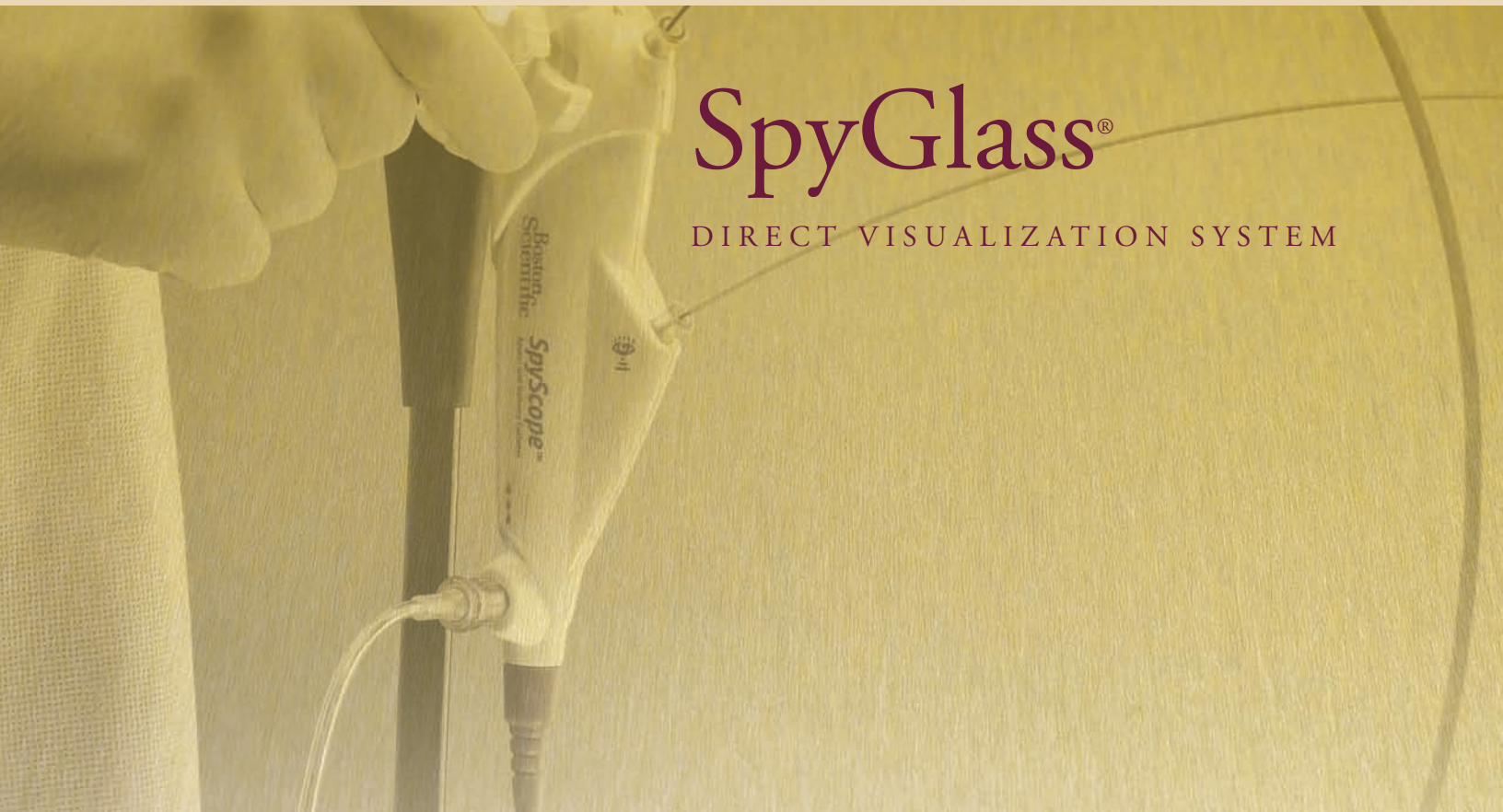
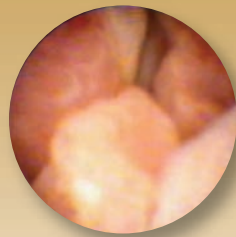
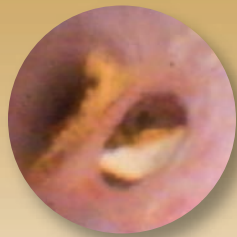
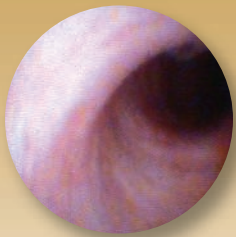




PANCREATICO-BILIARY IMAGE ATLAS



SpyGlass®

DIRECT VISUALIZATION SYSTEM

ATLAS OF CHOLANGIOSCOPY WITH THE SPYGLASS® SYSTEM



Douglas G. Adler, MD, FACG, FASGE

Director of Therapeutic Endoscopy, Assistant Professor of Medicine
Division of Gastroenterology and Hepatology
Huntsman Cancer Center, University of Utah School of Medicine, Salt Lake City, Utah

This collection of images obtained via the SpyGlass Cholangioscopy System is presented to help familiarize physicians with the appearance of some common biliary findings. Images of normal biliary ductal anatomy are presented to illustrate and familiarize the reader with the appearance of a healthy, normal bile duct and to contrast with the appearance of the biliary tree in a variety of pathologic states. Common conditions such as biliary stones, primary sclerosing cholangitis (with mild, moderate, and severe inflammation) as well as several images to illustrate the varying appearance of cholangiocarcinoma have been included.

HEALTHY

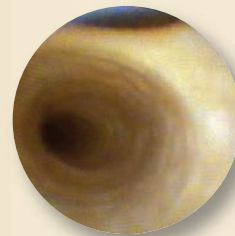


Figure 1
Normal duct wall with normal bifurcation.

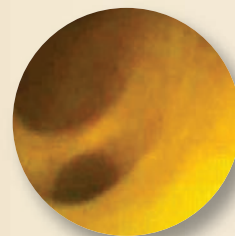


Figure 2
Cystic duct origin. The smaller lumen of the cystic duct is seen joining the common bile duct in this image. Note normal duct wall appearance.

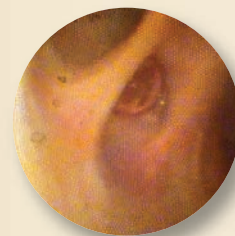


Figure 3
Normal duct wall with normal bifurcation.
Note air bubble in ductal opening.

ATLAS OF PANCREATOSCOPY WITH THE SPYGLASS® SYSTEM



Urban Arnelo, MD, PhD

Karolinska University Hospital
Stockholm, Sweden

The SpyGlass® Direct Visualization System constitutes a definite improvement of commercially existing endoscopes for peroral cholangioscopy and pancreatoscopy. The SpyGlass System can be used to discriminate in the differential diagnosis between chronic pancreatitis and ductal pancreatic carcinoma. It is particularly useful to diagnose and determine the extent of growth in IPMN and can further be used to differentiate some of the cystic lesions of the pancreas. It allows directed biopsy sampling and forms the basis for intraductal confocal microscopy.

HEALTHY

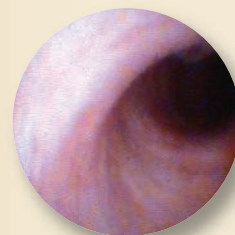


Figure 1
Normal pancreatic duct

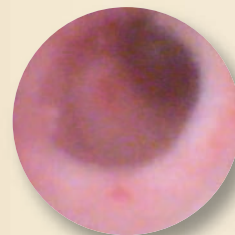


Figure 2
Normal pancreatic duct

BILIARY STONES

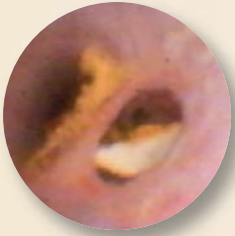


Figure 4
Classic Mirizzi's Syndrome with a stone lodged in the cystic duct.

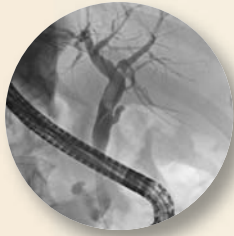


Figure 7
Cholangiogram demonstrating large, 2cm stone at the level of the biliary hilum.



Figure 5
Complete occlusion of duct due to various sized stones.



Figure 8
Same stone as in Figure 7 and 8 when viewed with SpyGlass Cholangioscope System just prior to electrohydraulic lithotripsy (EHL).

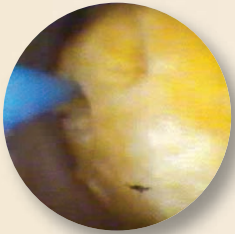


Figure 6
Stone disruption with holmium laser. Notice indentations on surface of stone from firing of laser.



Figure 9
Same stone as in Figure 7 after undergoing EHL. Note innumerable small stone fragments in bile duct lumen and EHL probe visible at the 2 O'clock position.



Figure 10
Cholangiogram of a patient with a mid-common bile duct cholangiocarcinoma.

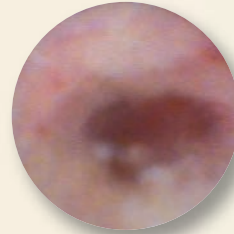


Figure 11
Same patient as in Figure 10. Cholangioscopic appearance of cholangiocarcinoma. Note circumferential stricture with visible tumor.

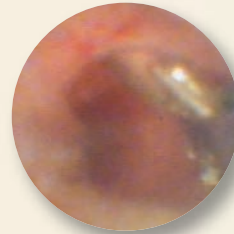


Figure 12
SpyBite® Biopsy Forceps in cholangiocarcinoma patient with PSC. Biopsy report revealed malignant tissue.

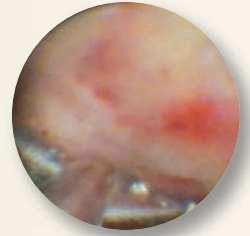


Figure 13
Cholangiocarcinoma in a patient with a completely obstructed left hepatic duct. Note the erythematous ulcerated appearance of the lesion. The lesion is undergoing biopsy with a SpyBite Forceps in this image as well.

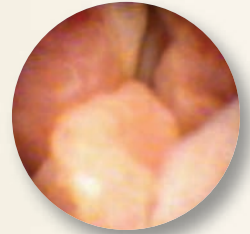


Figure 14
Biopsy of the polyps with SpyBite Biopsy Forceps came back positive for biliary papillomatosis and the patient underwent a liver resection.

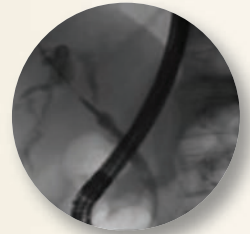


Figure 15
Stricture can be seen fluoroscopically in proximal portion of duct. Note location of SpyScope® Delivery Catheter within the stricture.

PANCREATIC STONE

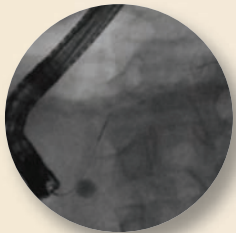


Figure 3
A 9 mm stone in the MPD close to the papilla, and a guide wire in the MPD



Figure 5
Pancreatic stone debris



Figure 7
A guide wire left in MPD during the SpyGlass System session



Figure 9
View from inside of pseudocyst with calcifications within the cyst wall



Figure 11
Calcifications within dilated MPD



Figure 4
Intraductal view of the stone

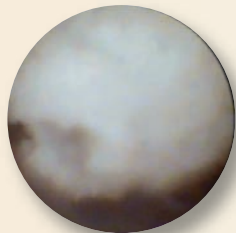


Figure 6
Pancreatic stone debris



Figure 8
Pancreatogram is showing severe chronic pancreatitis + pseudocyst (black arrows) and parenchymal calcifications

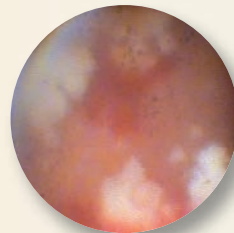


Figure 10
Closer view of Figure 9

CARCINOMA

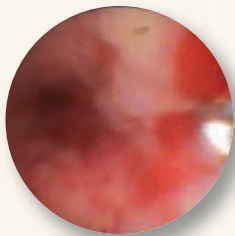


Figure 16
Nodular mucosa with villous fronds and mucin containing material. Note location of SpyBite Biopsy Forceps in duct.

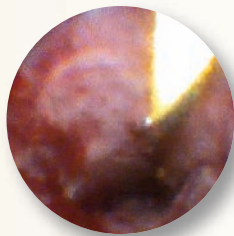


Figure 19
Distal Common Bile Duct Stricture caused by invasive pancreatic mass

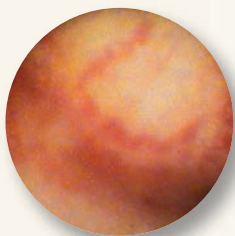


Figure 17
Fluoro showed a stricture that had a "fibrotic" appearance due to its resistance to a balloon. The SpyGlass System was used and confirmed a malignant Klatskin tumor.

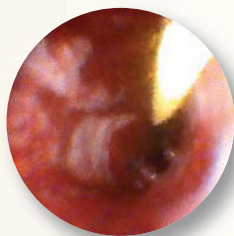


Figure 20
Mid Common Bile Duct Stricture caused by invasive pancreatic mass

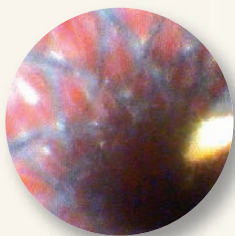


Figure 18
Post placement view of interior lumen of WallFlex® Biliary RX Fully Covered Stent confirmed placement over the tumor and revealed that the stent covering aided in stent patency.

PSC

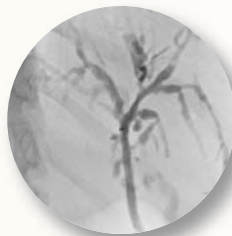


Figure 21
Cholangiogram demonstrating a patient with mild Primary Sclerosing Cholangitis (PSC). Note beading and pruning of intrahepatic ducts as well as irregular extrahepatic duct walls.

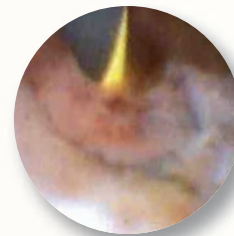


Figure 24
Same patient as in Figure 23. Severe duct wall inflammation with non-obstructing stricture.

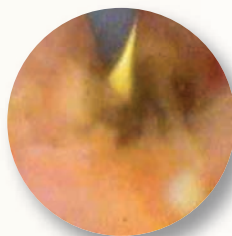


Figure 22
Mild biliary duct wall inflammation in a patient with mild PSC. Note erythematous changes and "boggy" appearance of duct walls.

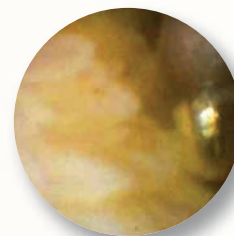


Figure 25
SpyBite Biopsy Forceps of papillary projections. Biopsy report was consistent with benign inflammation.



Figure 23
Cholangiogram in a patient with severe PSC. Note marked pruning of intrahepatic ducts and dominant stricture in left hepatic duct.

IPMN



Figure 12
Fingerlike protrusions which are typical of IPMN.

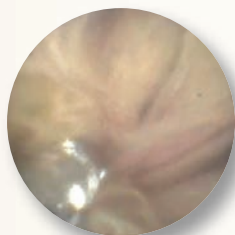


Figure 14
Pathology of IPMN captured with SpyBite Biopsy Forceps.

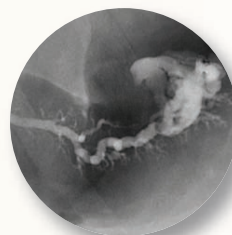


Figure 16
Same patient as in Figure 14 and 15. Mucus prevents clear view from inside the dilated portion of MPD. Multiple SpyBite biopsies are suggestive of IPMN. The patient was operated with a total pancreatectomy, histopathology show multifocal IPMN.



Figure 13
Pancreatoduodenal fistula

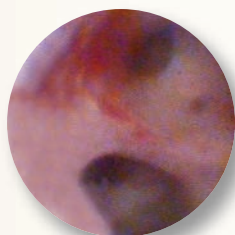


Figure 15
Same patient as Figure 14. Intraductal view, approaching the dilated portion of the MPD. Dilated side branches are also seen.

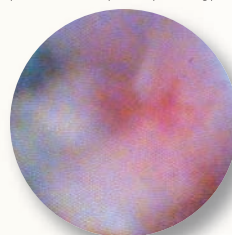
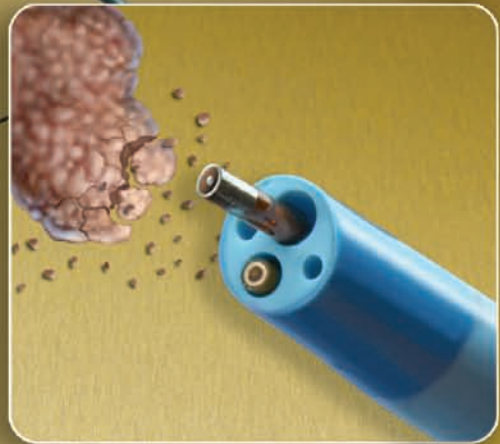


Figure 17
Same patient as in Figure 16. Suspected IPMN, mucus prevents clear view. The patient was operated with a total pancreatectomy, histopathology showed multifocal IPMN.



A difference you can see.™

Images courtesy of:

- Dr. Douglas Adler, University of Utah School of Medicine, UT
- Dr. Urban Arnelo, Karolinska University Hospital, Stockholm, Sweden
- Dr. Markus Goldschmiedt, Medical Center of Plano, TX
- Dr. Bora Gumastop, St. Peter's Hospital, NY
- Dr. Kadirawelpillai Iswara, Maimonides Hospital, NY
- Dr. Syed Faisal Jafri, Menorah Medical Center, MD
- Dr. Pankaj J. Patel, Florida Hospital Heartland Division, FL
- Dr. Sandeep Patel, University of Texas Health & Sciences Center, TX
- Dr. Ed Schafer, The Nebraska Medical Center, NE
- Dr. Adam Slivka, University of Pittsburgh Medical Center, PA

Boston Scientific

Delivering what's next.™

Boston Scientific Corporation
One Boston Scientific Place
Natick, MA 01760-1537
www.bostonscientific.com

Ordering Information
1.800.225.3226

© 2010 Boston Scientific Corporation
or its affiliates. All rights reserved.

SME15390 1.5M February 2010